

ORIGINAL PAPER

Heterogeneous Entity Representation for Medicinal Synergy Prediction

Jiawei Wu,¹ Jun Wen,^{2,3} Mingyuan Yan,¹ Anqi Dong⁴ and Can Chen^{5,6,*}

¹School of Medicine, National University of Singapore, Singapore 119077, ²Harvard Medical School, Harvard University, Boston, MA 02115, USA, ³VA Boston Healthcare System, MA 02115, USA, ⁴Department of Mechanical and Aerospace Engineering, University of California, Irvine, Irvine, CA 92697, USA, ⁵School of Data Science and Society, University of North Carolina at Chapel Hill, Chapel Hill, NC 27599, USA and ⁶Department of Mathematics, University of North Carolina at Chapel Hill, Chapel Hill, NC 27599, USA

*Corresponding author.

FOR PUBLISHER ONLY Received on Date Month Year; revised on Date Month Year; accepted on Date Month Year

Abstract

Motivation: Medicinal synergy prediction is a powerful tool in drug discovery and development that harnesses the principles of combination therapy to enhance therapeutic outcomes by improving efficacy, reducing toxicity, and preventing drug resistance. While a myriad of computational methods has emerged for predicting synergistic drug combinations, a large portion of them may overlook the intricate, yet critical relationships between various entities in drug interaction networks, such as drugs, cell lines, and diseases. These relationships are complex and multidimensional, requiring sophisticated modeling to capture nuanced interplay that can significantly influence therapeutic efficacy.

Results: We introduce a salient deep hypergraph learning method, namely, Heterogeneous Entity Representation for Medicinal Synergy prediction (HERMES), to predict anti-cancer drug synergy. HERMES integrates heterogeneous data sources, encompassing drug, cell line, and disease information, to provide a comprehensive understanding of the interactions involved. By leveraging advanced hypergraph neural networks with gated residual mechanisms, HERMES can effectively learn complex relationships/interactions within the data. Our results show HERMES demonstrates state-of-the-art performance, particularly in forecasting new drug combinations, significantly surpassing previous methods. This advancement underscores the potential of HERMES to facilitate more effective and precise drug combination predictions, thereby enhancing the development of novel therapeutic strategies.

Availability: The source code is publicly available at <https://github.com/Christina327/HERMES>.

Contact: canc@unc.edu

1. Introduction

Exploring drug combinations leads a promising avenue for enhancing cancer treatment efficacy while minimizing toxicity and adverse reactions in modern medicine (Jia et al., 2009; Csermely et al., 2013). Combination therapies, involving multiple drugs administered as a single treatment regimen, offer potential benefits over traditional single-drug approaches, particularly under cancer and tumor treatment contexts (Chou, 2006; O’Neil et al., 2016). Not only do they hold the promise of greater therapeutic efficacy, but present an opportunity to mitigate host toxicity and unwanted side effects, as the doses of drug combinations are often sub-mutagenic compared to individual drug doses. However, optimizing drug combinations can be challenging, as poorly chosen combinations may lead to adverse effects and sub-optimal outcomes (Hecht et al., 2009; Tol et al., 2009). Thus, there is a critical need to identify precise synergistic drug pairs tailored to different cancer types.

Historically, the identification of effective combination drugs relied on clinical experience, a process that is not only time-consuming and resource-intensive but also prone to trial and error. In contrast, high-throughput screening has emerged as an affordable and efficient strategy for identifying synergistic drug pairs, leading to the generation of extensive datasets (O’Neil et al., 2016; Holbeck et al., 2017; Jaaks et al., 2022). However, certain limitations persist, such as the inability of cancer cell lines to accurately represent *in vivo* states and the impracticality of exhaustively testing all members of the full combinatorial space with high-throughput screening (Ferreira et al., 2013; Goswami et al., 2015; Morris et al., 2016).

Recently, numerous computational methods for predicting drug synergy have been proposed. Pioneering methods, including DeepSynergy (Preuer et al., 2018) and Matchmaker (Kuru et al., 2021), utilize deep neural networks with both the chemical properties of drugs and the gene expression profiles of cell lines. The deep tensor factorization model (Sun et al., 2020) combines tensor decomposition with neural networks to forecast the synergistic effects of drug combinations. Additionally,

TransSynergy (Liu and Xie, 2021) adopts a transformer network model using drug-target and protein-protein interaction data. DeepDDS (Wang et al., 2022) employs graph convolutional networks (GCNs) (Wu et al., 2020) and multi-layer perceptrons (MLP) for synergy prediction. The current state-of-the-art method HypergraphSynergy (Liu et al., 2022) made strides in this direction by incorporating hypergraph neural networks (HGNNs) (Feng et al., 2019; Bai et al., 2021) to model these dynamics in a more interconnected and multifaceted manner. Hypergraphs generalize graphs by allowing hyperedges to connect more than two nodes (Chen and Rajapakse, 2020; Chen et al., 2021; Pickard et al., 2023), encode multidimensional (or high-order) correlations and connections. However, HypergraphSynergy has notable limitations in fully capturing the intricate nature of these interactions. More importantly, its ability to generalize, especially in the context of novel drug combinations, remains a challenge.

In this article, we propose a novel deep hypergraph learning method – Heterogeneous Entity Representation for MEDicinal Synergy prediction (HERMES) – to enhance drug synergy prediction. HERMES distinguishes itself with its innovative strategy for integrating a variety of data sources, including drug chemical properties, cell line gene expressions, and interactions between drugs and indications. This integration is achieved through a heterogeneous hypergraph structure, which aids in assimilating extensive prior knowledge and enhances the model’s ability to generalize in novel contexts. Another notable breakthrough of HERMES is addressing the widespread issue of over-smoothing in message-passing networks (Li et al., 2018) by implementing a gated residual mechanism, which not only retains more information but also notably enhances the expressiveness of the network. Our empirical results highlight HERMES’s effectiveness, especially in novel scenarios, significantly surpassing HypergraphSynergy and establishing it as a leading solution. The key contributions of this article are (1) integration of varied knowledge sources (including drugs, cell lines, and diseases) into a scalable and heterogeneous model architecture; (2) enhancement of message passing over hypergraphs with gated residual mechanisms for augmented network expressiveness; (3) empirical evidence showcasing

superior performance compared to previous methods, with a particular emphasis on robust generalization in novel contexts.

This article is structured into four sections. The main architecture of HERMES is detailed in Section 2. We assess the performance of HERMES (along with other representative drug synergy prediction methods) including a comprehensive ablation study in Section 3. Finally, we conclude by discussing future research directions in Section 4.

2. Materials and Methods

2.1. Overview of HERMES

Our framework conceptualizes drug synergy prediction under a hypergraph framework, treating it as a hyperedge prediction problem, where drugs, cell lines, and diseases are represented by nodes while synergistic drug–drug–cell line triplets and drug-disease pairwise relations are represented by hyperedges. Hyperedge prediction is a generalization of edge prediction on graphs (Chen and Liu, 2023; Chen et al., 2023). This innovative approach unfolds through three interconnected phases: initialization, refinement, and consolidation (Figure 1). Each phase plays a pivotal role in processing and integrating varied data types, thereby synthesizing comprehensive information crucial for accurate drug synergy predictions. Drawing inspiration from HypergraphSynergy, our model introduces novel methodologies and integrates cutting-edge techniques to significantly enhance prediction accuracy and reliability at each phase of analysis.

2.2. Feature Initialization

The initialization phase is crucial in our synergy prediction methodology, as it involves acquisition of initial features for drugs, cell lines, and diseases. This phase is pivotal in not only gathering diverse data but ensuring these features are transformed to a uniform dimensionality, which is fundamental for the subsequent analyses in our hypergraph model.

Drug features. We generate drug features by utilizing molecular graphs, which are built from the Simplified Molecular Input Line Entry System (SMILES) representations of drugs

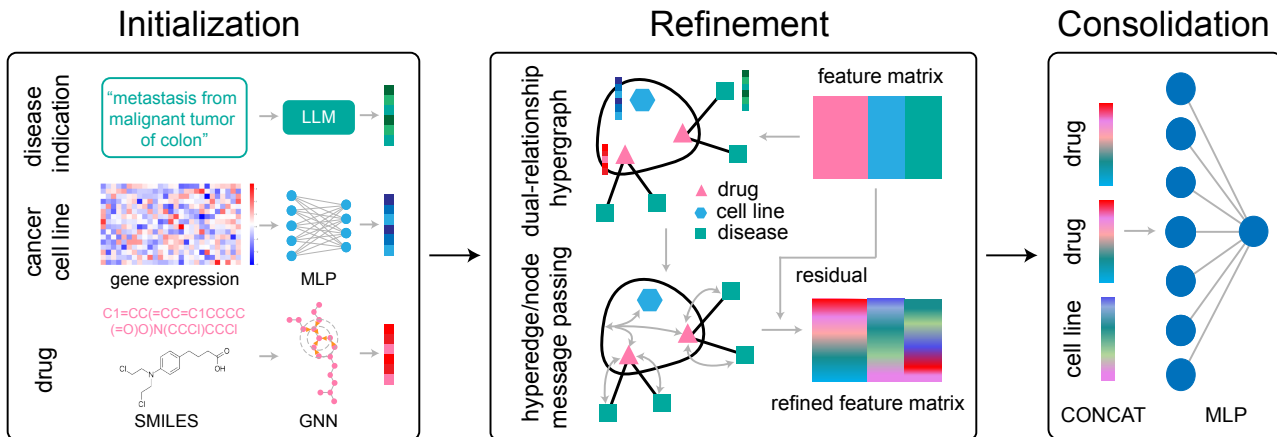


Fig. 1. Overview of HERMES framework. HERMES has three key phases: (1) initialization: acquiring and transforming initial features of drugs, cell lines, and disease indications to a uniform dimensionality; (2) refinement: enhancing feature representations through the construction of a dual-relationship hypergraph and the application of hypergraph neural networks with gated residual connections; (3) consolidation: integrating refined features using a binary classification model to predict drug synergies with high accuracy. Each phase is integral to the framework’s ability to process diverse data types and generate precise drug synergy predictions.

(Kim et al., 2019). By employing the ConvMolFeaturizer method from the DeepChem library (Duvenaud et al., 2015), we construct a molecular graph for each drug, with atoms represented as nodes and bonds as edges. Subsequently, we employ advanced graph transformer networks (GTNs) on molecular graphs to enhance the representations of atoms and drugs. Denote the feature vector of atom i as \mathbf{a}_i . The updated feature (denoted as \mathbf{a}'_i) through a GTN is then computed as

$$\mathbf{a}'_i = \sigma\left(\mathbf{W}_1\mathbf{x}_i + \sum_{j \in \mathcal{N}(i)} \alpha_{ij} \mathbf{W}_2\mathbf{a}_j\right), \quad (1)$$

where $\mathcal{N}(i)$ denotes the neighboring atoms of atom i , \mathbf{W}_1 and \mathbf{W}_2 are learnable weight matrices, and σ is a nonlinear activation function. Here, α_{ij} is the multi-head attention coefficient defined as

$$\alpha_{ij} = \text{Softmax}\left(\frac{(\mathbf{W}_3\mathbf{a}_i)^\top (\mathbf{W}_4\mathbf{a}_j)}{\sqrt{d}}\right),$$

where d is the latent size of each head, and \mathbf{W}_3 and \mathbf{W}_4 are learnable weight matrices. GTNs can effectively capture and model complex relationships and interactions within graph-structured data by assigning attention scores to neighboring nodes, enabling a more targeted aggregation of information compared to traditional convolutional methods such as GCNs (Shi et al., 2020). Finally, we compute the feature vector of a drug by aggregating all its updated atom features using maximum pooling. The choice of maximum pooling is motivated by the fact that drug molecular graphs may vary in the number of atom nodes. The resulting feature matrix for all drugs is denoted as \mathbf{X}_{drug} .

Cell line features. We utilize gene expression profiles to generate cell line features. Following a log2 transformation and z-score normalization of gene expression data, we employ an MLP to derive the features for cell lines, ensuring uniform dimensionality with drug features. Denote the feature vector for cell line i by \mathbf{c}_i , the updated feature (denoted as \mathbf{c}'_i) through an MLP is computed as

$$\mathbf{c}'_i = \sigma(\mathbf{W}_5\mathbf{c}_i + \mathbf{b}_5), \quad (2)$$

where \mathbf{W}_5 and \mathbf{b}_5 are learnable weight matrix and a bias vector, respectively. The resulting feature matrix for all cell lines is denoted as \mathbf{X}_{cell} .

Disease features. We create disease features by leveraging a novel embedding method called CODER, a knowledge-graph-guided large language model for cross-lingual medical term representation using contrastive learning (Yuan et al., 2022). CODER excels in providing close vector representations for various terms representing similar medical concepts in multiple languages, making it particularly beneficial for extracting enriched and contextually relevant disease features (Yuan et al., 2022). Similar to cell line features processing, we employ an MLP on the obtained disease features to align with the consistent dimensionality of drug and cell line features. The resulting feature matrix for all diseases is denoted as \mathbf{X}_{dis} . Notably, integrating CODER with disease information enhances our model’s ability to comprehend the intricate relationships between drugs, cell lines, and diseases within the hypergraph framework.

2.3. Feature Refinement

In the refinement phase, we focus on transforming the obtained drug, cell line, and disease features into contextually

enriched representations. This process is achieved through the construction of a dual-relation hypergraph and the implementation of an advanced feature enhancement technique, namely HGNNs with gated residual connections. These elements collectively elevate our model’s ability to identify complex interrelationships, setting the stage for more precise synergy predictions.

Hypergraph construction. We construct a novel dual-relationship hypergraph involving relationships between drugs, cell lines, and diseases. The hypergraph contains two types of hyperedges: (1) drug-drug-cell line triplets (third-order interactions), which capture the potential synergistic effects between specific drugs and cell lines; (2) drug-disease relationship (pairwise interactions or traditional edges), which represents associations between drugs and their indications (medical conditions they treat), providing insights into the therapeutic spectrum of drugs. This dual-relationship hypergraph, which has never been considered in previous methods, is pivotal in enriching the feature representations by integrating the various features of drugs, cell lines, and diseases.

Hypergraph neural networks. We employ advanced HGNNs with gated residual mechanisms to refine drug, cell lines, and disease features. HGNNs excel in capturing the complex relationships and interactions within the hypergraph, making it a pivotal component in our model for drug synergy prediction (Feng et al., 2019). Denote the feature matrix as $\mathbf{X} = \text{vercat}(\mathbf{X}_{\text{drug}}, \mathbf{X}_{\text{cell}}, \mathbf{X}_{\text{dis}})$ where vercat is the vertical concatenation operation. The refined features (denoted as \mathbf{X}') through an HGNN are computed as

$$\mathbf{X}' = \sigma(\mathbf{D}^{-1}\mathbf{H}\mathbf{E}^{-1}\mathbf{H}^\top\mathbf{X}\mathbf{W}_6), \quad (3)$$

where \mathbf{D} and \mathbf{E} are diagonal matrices of node and hyperedge degrees, respectively. \mathbf{H} is the incidence matrix of the hypergraph, containing binary values to indicate the presence or absence of any node in any hyperedge, and \mathbf{W}_6 is learnable weight matrix. Here, the superscripts -1 and \top denote matrix inversion and transposition, respectively. To enhance the expressive capacity of our network and extract more intricate patterns from the hypergraph, we increase the number of layers in the HGNN. However, this approach leads to a well-known challenge in graph neural networks, i.e., over-smoothing (Cai and Wang, 2020).

The phenomenon of over-smoothing occurs when the network layers become too deep, leading to the homogenization of node features and a loss of valuable information. To mitigate this issue and further empower our network’s expressive capabilities, we introduce a novel solution using gated residual connections (Li et al., 2018). The implementation of gated residual connections within an HGNN is defined as

$$\mathbf{X}' = \mathbf{X} + \sigma\left(\mathbf{W}_7\sigma(\mathbf{D}^{-1}\mathbf{H}\mathbf{E}^{-1}\mathbf{H}^\top\mathbf{X}\mathbf{W}_6) + \mathbf{b}_7\right)\mathbf{X}, \quad (4)$$

where \mathbf{W}_7 and \mathbf{b}_7 are learnable weight matrix and bias vector of the gate, respectively. The introduction of the gated residual connection in HGNNs allows our neural network to dynamically regulate the integration of original and convoluted features, which significantly reduces the risk of over-smoothing by providing a controlled blending of features. Additionally, we implement the equilibrium bias initialization (EBI) strategy (Wang et al., 2010), where we initialize \mathbf{b}_7 with a relatively negative value. The EBI strategy ensures that the gate functions close to an identity operation at the start of training, allowing for gradual and more effective feature integration.

Our refinement approach utilizing HGNNs coupled with gated residual connections significantly enhances the model’s ability to discern complex patterns and interactions between drugs, cell lines, and diseases, thereby creating more accurate representations for them compared to previous methods such as HypergraphSynergy.

2.4. Feature Consolidation

In the consolidation phase, our primary objective is to produce predictive insights by integrating the refined features obtained from the earlier phase. We employ a binary classification model that uses the features refined over the dual-relationship hypergraph to identify drug synergies. It classifies the interactions between drug combinations and cell lines into two categories: synergistic and non-synergistic, which provides a clear, binary output for each potential drug synergy scenario.

Predictive model. The essence of the consolidation phase is using a predictive model that leverages the features obtained in the refinement phase to evaluate the potential synergistic effects of drug combinations on specific cell lines and their implications for disease treatment. Suppose the final refined features of drug i , drug j , and cell line k are denoted by $\tilde{\mathbf{d}}_i$, $\tilde{\mathbf{d}}_j$, and $\tilde{\mathbf{c}}_k$, respectively. The synergy score (denoted as S) can be computed using an MLP, i.e.,

$$S = \sigma(\mathbf{W}_s \text{vercat}(\tilde{\mathbf{d}}_i, \tilde{\mathbf{d}}_j, \tilde{\mathbf{c}}_k) + \mathbf{b}_s), \quad (5)$$

where \mathbf{W}_s and \mathbf{b}_s are a learnable weight matrix and a bias vector, respectively.

To address the unordered nature of drug pairs, a critical aspect in synergy prediction, we implement a pairwise symmetric permutation augmentation strategy (Zhou et al., 2024). This approach involves presenting both permutations of each drug pair in our dataset. For example, if a data sample includes the combination (drug1, drug2, cell line), we also introduce (drug2, drug1, cell line) as a distinct sample. This augmentation is essential to ensure that our model is agnostic to the order of drugs, enhancing its capability to uniformly recognize synergy.

Model training. Given the binary nature of our prediction task, we utilize the cross-entropy loss function (Mao et al., 2023), a standard and effective choice for binary classification models defined as

$$\text{Loss} = -\frac{1}{N} \sum_{i=1}^N [y_i \log(\hat{y}_i) + (1 - y_i) \log(1 - \hat{y}_i)], \quad (6)$$

where y_i and \hat{y}_i represent the actual and predicted label (synergistic or non-synergistic) of the i th sample, respectively, and N is the total number of samples. The model is trained on a dataset consisting of drug pairs, cell lines, and their corresponding synergy labels. The training process involves adjusting the weights of the neural network to minimize the cross-entropy loss, enhancing the model’s ability to accurately classify drug synergies.

2.5. HERMES and HypergraphSynergy

Although HERMES is inspired by HypergraphSynergy, it significantly diverges from HypergraphSynergy in the following aspects:

- HERMES integrates an additional knowledge source of diseases and constructs a dual-relationship hypergraph.

- HERMES leverages advanced GTNs to obtain drug features, while HypergraphSynergy only utilizes traditional GCNs.
- HERMES improves HGNNs during the refinement phase by incorporating gated residual mechanisms to address the issue of over-smoothing.
- HERMES exploits useful learning techniques such as EBI and pairwise symmetric permutation augmentation to enhance the model’s learning ability.

Below, we show that HERMES significantly outperforms HypergraphSynergy in two drug synergy datasets, especially under the context of predicting new drug combinations.

3. Experiments

3.1. Datasets

We collected four categories of data, including drug synergy data, molecular information for drugs, genomic characteristics of cancer cell lines, and indications for drug therapy in diseases, from multiple publicly available databases. The details of these data are listed as follows:

- **Drug synergy datasets:** We gathered data on the synergy of anti-cancer drugs from two prominent large-scale tumor screening datasets - the O’Neil dataset (O’Neil et al., 2016) and the NCI-ALMANAC dataset (Holbeck et al., 2017). The O’Neil dataset comprises 23,062 samples involving 38 unique drugs and 39 distinct human cancer cell lines. Each sample measures Loewe synergy scores for two drugs in combination with a specific cell line. The NCI-ALMANAC dataset contains 304,549 samples, including ComboScores for 104 FDA-approved drugs in pairings across the NCI-60 cell line panel.
- **Drug molecular structures:** Information on the SMILES of drugs is obtained from the PubChem database (Kim et al., 2019).
- **Gene expression in cancer cell lines:** Data on gene expression in cancer cell lines are sourced from the Cell Lines Project within the COSMIC database (Forbes et al., 2015). In this context, we specifically considered the expression values of 651 genes related to the COSMIC cancer gene census. These expression values are subjected to logarithmic (\log_2) transformation and z-score normalization.
- **Indications for drug therapy in diseases:** The indication dataset is sourced from PrimeKG (Chandak et al., 2023), a multi-modal knowledge graph designed to support precision medicine. PrimeKG integrates data from 20 high-quality biomedical resources, including DisGeNET and DrugBank. It provides detailed relationships between drugs and diseases, covering indications, contraindications, and off-label uses. This dataset captures how drugs target disease-associated molecular perturbations, facilitating analyses in drug repurposing and therapeutic strategies

We performed a comprehensive data preprocessing on two primary drug synergy datasets – NCI-ALMANAC and O’Neil. To ensure the quality and relevance of the data, we excluded cell lines lacking gene expression information and drugs without SMILES details. Following this preprocessing phase, the NCI-ALMANAC dataset comprises 74,139 measurement samples of ComboScores for 87 drugs across 55 cancer cell lines, while the O’Neil dataset encompasses 18,950 samples of Loewe synergy scores for 38 drugs and 39 cancer cell lines (Table 1). Subsequently, we removed drugs from the ‘drug-disease

Table 1. Statistics of the two datasets.

Dataset	#Drugs	#Targets	#Samples
NCI-ALMANAC	87	55	74139
O’Neil	38	39	18950

dataset’ that are not present in the aforementioned drug synergy datasets. This led to the extraction of indications for 111 diseases corresponding to 111 drugs within the NCI-ALMANAC dataset and 222 diseases corresponding to 222 drugs within the O’Neil dataset.

3.2. Baselines

We conducted a comparative analysis of our approach with representative drug synergy prediction techniques. Below is a brief overview of each of the baseline methods:

- **DeepSynergy (Preuer et al., 2018):** It utilizes a three-layer feedforward neural network to predict synergy scores, incorporating gene expression as cell line features and three types of chemical descriptors as drug features.
- **DTF (Sun et al., 2020):** It extracts latent features from the drug synergy matrix through tensor factorization and employs them to train a deep neural network model for predicting drug synergy.
- **HypergraphSynergy (Liu et al., 2022) (the current state-of-the-art method):** It formulates synergistic drug combinations across cancer cell lines as a hypergraph. In this hypergraph, drugs and cell lines are represented by nodes, while synergistic drug–drug–cell line triplets are represented by hyperedges. It leverages the biochemical features of drugs and cell lines as node attributes. Additionally, a HGNN is employed to learn drug and cell line embeddings from the hypergraph and predict drug synergy.

3.3. Experiment Setup

In this study, each dataset is initially divided into two distinct sets: a training set, accounting for 90% of the total data, and a test set comprising the remaining 10%. The training set undergoes a rigorous five-fold cross-validation process. This process is structured in three unique partitioning strategies to ensure comprehensive evaluation:

- **Random:** Samples are randomly divided, providing a baseline assessment of model performance.
- **Target:** Samples are stratified by target cell line, ensuring each fold’s validation set contains unique cell lines not present in its training set.
- **DrugComb:** Samples are stratified based on drug combinations. Each validation set included drug combinations not seen in the training set, although individual drugs might overlap.

The test set is used for final evaluation, whereby an unbiased assessment of the model’s predictive power is ensured.

Additionally, for the classification task, synergy scores are converted to binary outcomes. Following established protocols (Preuer et al., 2018; Sun et al., 2020), a threshold of 30 is used. Scores above this threshold indicate a positive synergy, while scores below are deemed negative. Ultimately, the model’s performance is evaluated using key metrics: area under the receiver operating characteristic curve (AUROC) and area under the precision-recall curve (AUPRC). Both metrics

Table 2. Hyperparameter selection (Selected hyperparameters are highlighted in bold.)

Hyperparameter	Values
learning rate	{1e-3, 5e-4, 2e-4 , 1e-4, 5e-5, 2e-5}
weight decay	{1e-1, 1e-2 , 1e-3, 1e-4}
attention heads	{2, 4 , 8}
refinement layer	{2, 3 , 4}
interaction weight	{0, 0.02 , 0.05, 0.1, 0.2, 0.5, 1.0}

provide comprehensive view of the model’s effectiveness in precision and recall aspects.

3.4. Hyperparameters

To optimize the performance of our model, we conducted a grid search to fine-tune hyperparameters such as the refinement layer and learning rate. Table 2 presents the range of values considered for each hyperparameter. The optimal values (in bold) are selected based on their performance during the training and validation phases.

3.5. Performance Comparison and Analysis

In the NCI-ALMANAC dataset, HERMES exhibits superior performance across all evaluation strategies compared to the baseline methods (Figure 2A). Under the random partitioning strategy, HERMES achieves an AUROC of 85.91%, which is significantly higher than HypergraphSynergy, DTF, and DeepSynergy, which score 85.30%, 82.38%, and 83.50%, respectively (HERMES vs. HypergraphSynergy: p -value < 0.05, two-sample t -test). In the more challenging ‘DrugComb’ mode, HERMES achieves an AUROC of 79.75%, significantly outperforming the other methods, with HypergraphSynergy recording 77.98% (p -value < 0.01, two-sample t -test), and DTF and DeepSynergy achieving even lower scores. For the ‘Target’ mode, HERMES still performs better than the rest of the methods. Additionally, the AUPRC results reflect a similar trend (right panel).

The performance of HERMES is further validated using the ONEIL dataset (Figure 2B), and similar results are observed across the three modes in terms of AUROC and AUPRC. In the random stratification, HERMES attains an AUROC of 93.67%, significantly outperforming HypergraphSynergy, DTF, and DeepSynergy, which score 92.30%, 91.38%, and 90.60%, respectively (HERMES vs. HypergraphSynergy: p -value < 0.001, two-sample t -test). In the ‘DrugComb’ mode, HERMES maintains a competitive edge with an AUROC of 88.34%, significantly surpassing HypergraphSynergy at 86.22% (p -value < 0.05, two-sample t -test). HERMES also achieves better performance under the ‘Target’ mode compared to the other methods.

To further validate the performance of our model, we considered two new validation modes using the ALMANAC dataset (which contains more samples) to test the model’s generalization ability to previously unseen drugs. The two modes are defined as follows: (1) **DrugSingle** where samples are stratified based on individual drugs, with one drug in each drug combination in the validation set being novel to the training set. This approach reduces the dataset size and challenges the model to predict synergies involving new drugs; (2) **DrugDouble** where samples are stratified such that each drug combination in the validation set contains two drugs, neither of which appears in the training set, further reducing the dataset size and increasing the difficulty.

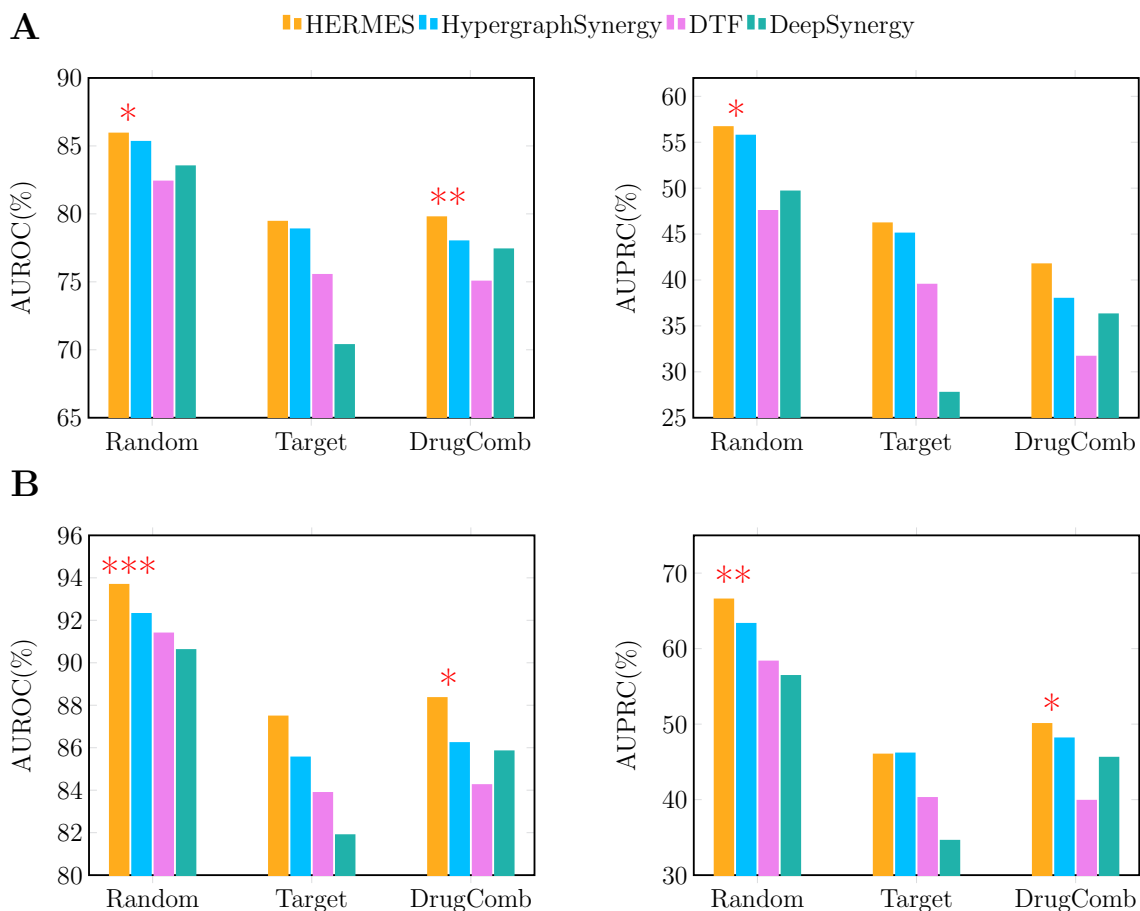


Fig. 2. Model performance comparison for (A) ALMANAC Dataset and (B) ONeil Dataset. The left panels shows the AUROC (%) scores for different models across three validation modes (Random, Target, DrugComb). The right panels present the AUPRC (%) scores for the same models and validation modes. (B) ONeil Dataset. Red asterisks indicate statistical significance between HERMES and HypergraphSynergy (** p -value < 0.001; ** p -value < 0.01; * p -value < 0.05; two-sample t -test).

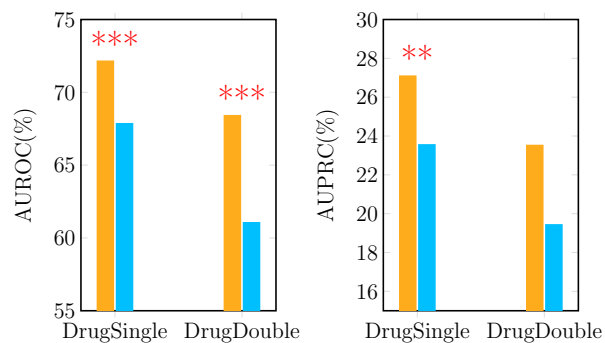


Fig. 3. Performance comparison of HERMES and HypergraphSynergy in the DrugSingle and DrugDouble modes using the ALMANAC dataset. Red asterisks indicate statistical significance between HERMES and HypergraphSynergy (** p -value < 0.001; ** p -value < 0.01; two-sample t -test).

The results of ‘DrugSingle’ and ‘DrugDouble’ are shown in Figure 3. In the ‘DrugSingle’ mode, HERMES achieves an AUROC of 72.13%, which is extremely significantly higher than HypergraphSynergy’s 67.84% (p -value < 0.001, two-sample t -test). Similarly, in the ‘DrugDouble’ mode, HERMES

scores an AUROC of 68.39%, highly significantly outperforming HypergraphSynergy (p -value < 0.001, two-sample t -test). The AUPRC metrics also show a consistent advantage for HERMES.

The comprehensive evaluation across different datasets and validation modes underscores the efficacy of HERMES in drug synergy prediction. The model consistently outperforms baseline methods in both AUROC and AUPRC metrics, demonstrating robust performance even in challenging scenarios. The results validate the superiority of HERMES in handling diverse drug synergy prediction tasks, emphasizing its importance for predicting untested drug synergies in clinical applications.

3.6. Ablation Study

The ablation study, as detailed in Table 3, scrutinizes the contributions of various components within the HERMES model utilizing the NCI-ALMANAC dataset. The evaluation encompasses three distinct modes: ‘Random’, ‘Target’, and ‘DrugComb’, with the primary metric being the average test AUROC for each configuration. The benchmark performance of the complete HERMES model registers an AUROC of 85.9% in the ‘Random’ mode, 79.4% in the ‘Target’ mode, and 79.8% in the ‘DrugComb’ mode. These figures establish the baseline

Table 3. Ablation study results. Average test AUROC of HERMES with and without key components.

Strategy	Random	Target	DrugComb
HERMES	85.9%	79.4%	79.8%
w/o transformer	82.8%	78.5%	78.3%
w/o disease	85.7%	79.2%	79.5%
w/o gated residual	84.0%	79.0%	78.8%
w/o gate	82.5%	78.7%	78.5%
w/o weighted hyperedge	82.8%	78.6%	78.5%

for assessing the impact of systematically removing specific components.

Contribution of transformer architecture. Excluding the transformer component results in significant performance drops across all three modes. These findings highlight the indispensable role of the transformer in capturing intricate relationships within the data.

Impact of disease knowledge. The exclusion of disease knowledge demonstrates a slight yet notable impact on the model’s performance. These findings suggest that incorporating disease knowledge provides a performance advantage, but the margin is relatively narrow. Future work could explore more sophisticated methods of integrating disease knowledge to potentially amplify this performance benefit.

Role of gated residuals. Omitting the gated residual connections results in a notable performance degradation, particularly in the ‘Random’ mode. This emphasizes the significance of gated residuals in maintaining high predictive accuracy, especially in scenarios with higher data variability.

Importance of gating mechanisms. The removal of the gating mechanism induces the most pronounced decline in performance across all modes. This underscores the critical function of gating mechanisms in modulating information flow and enhancing the model’s resilience.

Effect of weighted hyperedges. The absence of weighted hyperedges also leads to considerable performance decline across all three modes. This underscores the necessity of weighted hyperedges for accurately modeling complex interactions, particularly in the diverse Random mode.

In summary, the ablation study clearly demonstrates that each component of the HERMES model contributes uniquely to its overall efficacy. Transformer architecture, disease knowledge, gated residuals, gating mechanisms, and weighted hyperedges collectively enhance the model’s predictive performance. These results affirm the sophisticated design of HERMES, showcasing the synergistic effect of its components in achieving superior predictive accuracy across various validation strategies.

4. Conclusion

In this article, we introduced HERMES, a novel deep hypergraph learning method aimed at enhancing drug synergy prediction. By incorporating disease information and employing advanced GTNs and HGNNs with gated residual connections, HERMES achieves a superior performance on two drug synergy datasets compared to HypergraphSynergy and other methods. For future work, we will consider improving the scope of our analysis by incorporating a wider array of heterogeneous data sources such as target proteins, biological pathways, and therapeutic markers. We aim to bridge the gap between theoretical drug synergy prediction and practical clinical

applications, ultimately contributing to more effective and personalized treatment strategies.

References

- Bai, S., Zhang, F., and Torr, P. H. (2021). Hypergraph convolution and hypergraph attention. *Pattern Recognition*, 110:107637.
- Cai, C. and Wang, Y. (2020). A note on over-smoothing for graph neural networks. *arXiv preprint arXiv:2006.13318*.
- Chandak, P., Huang, K., and Zitnik, M. (2023). Building a knowledge graph to enable precision medicine. *Scientific Data*, 10(67).
- Chen, C., Liao, C., and Liu, Y.-Y. (2023). Teasing out missing reactions in genome-scale metabolic networks through hypergraph learning. *Nature Communications*, 14(1):2375.
- Chen, C. and Liu, Y.-Y. (2023). A survey on hyperlink prediction. *IEEE Transactions on Neural Networks and Learning Systems*.
- Chen, C. and Rajapakse, I. (2020). Tensor entropy for uniform hypergraphs. *IEEE Transactions on Network Science and Engineering*, 7(4):2889–2900.
- Chen, C., Surana, A., Bloch, A. M., and Rajapakse, I. (2021). Controllability of hypergraphs. *IEEE Transactions on Network Science and Engineering*, 8(2):1646–1657.
- Chou, T.-C. (2006). Theoretical basis, experimental design, and computerized simulation of synergism and antagonism in drug combination studies. *Pharmacological reviews*, 58(3):621–681.
- Csermely, P., Korcsmáros, T., Kiss, H. J., London, G., and Nussinov, R. (2013). Structure and dynamics of molecular networks: a novel paradigm of drug discovery: a comprehensive review. *Pharmacology & therapeutics*, 138(3):333–408.
- Duvenaud, D. K., Maclaurin, D., Iparraguirre, J., Bombarell, R., Hirzel, T., Aspuru-Guzik, A., and Adams, R. P. (2015). Convolutional networks on graphs for learning molecular fingerprints. *Advances in neural information processing systems*, 28.
- Feng, Y., You, H., Zhang, Z., Ji, R., and Gao, Y. (2019). Hypergraph neural networks. In *Proceedings of the AAAI conference on artificial intelligence*, volume 33, No.01, pages 3558–3565.
- Ferreira, D., Atega, F., and Chaves, R. (2013). The importance of cancer cell lines as in vitro models in cancer methylome analysis and anticancer drugs testing. *Oncogenomics and cancer proteomics-novel approaches in biomarkers discovery and therapeutic targets in cancer*, 1:139–166.
- Forbes, S. A., Beare, D., Gunasekaran, P., Leung, K., Bindal, N., Boutselakis, H., Ding, M., Bamford, S., Cole, C., Ward, S., et al. (2015). Cosmic: exploring the world’s knowledge of somatic mutations in human cancer. *Nucleic acids research*, 43(D1):D805–D811.
- Goswami, C. P., Cheng, L., Alexander, P., Singal, A., and Li, L. (2015). A new drug combinatory effect prediction algorithm on the cancer cell based on gene expression and dose–response curve. *CPT: Pharmacometrics & Systems Pharmacology*, 4(2):80–90.
- Hecht, J. R., Mitchell, E., Chidiac, T., Scroggin, C., Hagenstad, C., Spigel, D., Marshall, J., Cohn, A., McCollum, D., Stella, P., et al. (2009). A randomized phase iiib trial of chemotherapy, bevacizumab, and panitumumab compared

- with chemotherapy and bevacizumab alone for metastatic colorectal cancer. *Journal of Clinical Oncology*, 27(5):672–680.
- Holbeck, S. L., Camalier, R., Crowell, J. A., Govindharajulu, J. P., Hollingshead, M., Anderson, L. W., Polley, E., Rubinstein, L., Srivastava, A., Wilsker, D., et al. (2017). The national cancer institute almanac: a comprehensive screening resource for the detection of anticancer drug pairs with enhanced therapeutic activity. *Cancer research*, 77(13):3564–3576.
- Jaaks, P., Coker, E. A., Vis, D. J., Edwards, O., Carpenter, E. F., Leto, S. M., Dwane, L., Sassi, F., Lightfoot, H., Barthorpe, S., et al. (2022). Effective drug combinations in breast, colon and pancreatic cancer cells. *Nature*, 603(7899):166–173.
- Jia, J., Zhu, F., Ma, X., Cao, Z. W., Li, Y. X., and Chen, Y. Z. (2009). Mechanisms of drug combinations: interaction and network perspectives. *Nature reviews Drug discovery*, 8(2):111–128.
- Kim, S., Chen, J., Cheng, T., Gindulyte, A., He, J., He, S., Li, Q., Shoemaker, B. A., Thiessen, P. A., Yu, B., et al. (2019). Pubchem 2019 update: improved access to chemical data. *Nucleic acids research*, 47(D1):D1102–D1109.
- Kuru, H. I., Tastan, O., and Cicek, A. E. (2021). Matchmaker: a deep learning framework for drug synergy prediction. *IEEE/ACM transactions on computational biology and bioinformatics*, 19(4):2334–2344.
- Li, Q., Han, Z., and Wu, X.-M. (2018). Deeper insights into graph convolutional networks for semi-supervised learning. In *Proceedings of the AAAI conference on artificial intelligence*, volume 32, No.1.
- Liu, Q. and Xie, L. (2021). Transynergy: Mechanism-driven interpretable deep neural network for the synergistic prediction and pathway deconvolution of drug combinations. *PLoS computational biology*, 17(2):e1008653.
- Liu, X., Song, C., Liu, S., Li, M., Zhou, X., and Zhang, W. (2022). Multi-way relation-enhanced hypergraph representation learning for anti-cancer drug synergy prediction. *Bioinformatics*, 38(20):4782–4789.
- Mao, A., Mohri, M., and Zhong, Y. (2023). Cross-entropy loss functions: Theoretical analysis and applications. *arXiv preprint: 2304.07288*.
- Morris, M. K., Clarke, D. C., Osimiri, L. C., and Lauffenburger, D. A. (2016). Systematic analysis of quantitative logic model ensembles predicts drug combination effects on cell signaling networks. *CPT: pharmacometrics & systems pharmacology*, 5(10):544–553.
- O’Neil, J., Benita, Y., Feldman, I., Chenard, M., Roberts, B., Liu, Y., Li, J., Kral, A., Lejnine, S., Loboda, A., et al. (2016). An unbiased oncology compound screen to identify novel combination strategies. *Molecular cancer therapeutics*, 15(6):1155–1162.
- Pickard, J., Chen, C., Salman, R., Stansbury, C., Kim, S., Surana, A., Bloch, A., and Rajapakse, I. (2023). Hat: Hypergraph analysis toolbox. *PLOS Computational Biology*, 19(6):e1011190.
- Preuer, K., Lewis, R. P., Hochreiter, S., Bender, A., Bulusu, K. C., and Klambauer, G. (2018). DeepSynergy: predicting anti-cancer drug synergy with deep learning. *Bioinformatics*, 34(9):1538–1546.
- Shi, Y., Huang, Z., Feng, S., Zhong, H., Wang, W., and Sun, Y. (2020). Masked label prediction: Unified message passing model for semi-supervised classification. *arXiv preprint: 2009.03509*.
- Sun, Z., Huang, S., Jiang, P., and Hu, P. (2020). Dtf: deep tensor factorization for predicting anticancer drug synergy. *Bioinformatics*, 36(16):4483–4489.
- Tol, J., Koopman, M., Cats, A., Rodenburg, C. J., Creemers, G. J., Schrama, J. G., Erdkamp, F. L., Vos, A. H., van Groenigen, C. J., Sinnige, H. A., et al. (2009). Chemotherapy, bevacizumab, and cetuximab in metastatic colorectal cancer. *New England Journal of Medicine*, 360(6):563–572.
- Wang, H.-H., Klessen, R. S., Dullemond, C. P., Van Den Bosch, F. C., and Fuchs, B. (2010). Equilibrium initialization and stability of three-dimensional gas discs. *Monthly Notices of the Royal Astronomical Society*, 407(2):705–720.
- Wang, J., Liu, X., Shen, S., Deng, L., and Liu, H. (2022). Deepdds: deep graph neural network with attention mechanism to predict synergistic drug combinations. *Briefings in Bioinformatics*, 23(1):bbab390.
- Wu, Z., Pan, S., Chen, F., Long, G., Zhang, C., and Philip, S. Y. (2020). A comprehensive survey on graph neural networks. *IEEE transactions on neural networks and learning systems*, 32(1):4–24.
- Yuan, Z., Zhao, Z., Sun, H., Li, J., Wang, F., and Yu, S. (2022). Coder: Knowledge-infused cross-lingual medical term embedding for term normalization. *Journal of biomedical informatics*, 126:103983.
- Zhou, A., Yang, K., Burns, K., Cardace, A., Jiang, Y., Sokota, S., Kolter, J. Z., and Finn, C. (2024). Permutation equivariant neural functionals. *Advances in Neural Information Processing Systems*, 36.